Journal of Saudi Chemical Society (2023) **27**, 101683

King Saud University

Journal of Saudi Chemical Society

www.ksu.edu.sa
www.sciencedirect.com

ORIGINAL ARTICLE

Designing strategies towards non-fullerene DTCR1 based compounds for the exploration of non-linear optical behavior

Muhammad Khalid [a,b,*], Zubaria Saeed [a,b], Iqra Shafiq [a,b], Muhammad Adnan Asghar [c], Ataualpa Albert Carmo Braga [d], Saad M. Alshehri [e], Muhammad Safwan Akram [f,g], Suvash Chandra Ojha [h,*]

[a] *Institute of Chemistry, Khwaja Fareed University of Engineering & Information Technology, Rahim Yar Khan 64200, Pakistan*
[b] *Centre for Theoretical and Computational Research, Khwaja Fareed University of Engineering & Information Technology, Rahim Yar Khan 64200, Pakistan*
[c] *Department of Chemistry, Division of Science and Technology, University of Education, Lahore, Pakistan*
[d] *Departamento de Química Fundamental, Instituto de Química, Universidade de São Paulo, Av. Prof. Lineu Prestes, 748, São Paulo 05508-000, Brazil*
[e] *Department of Chemistry, College of Science, King Saud University, Saudi Arabia*
[f] *National Horizons Centre, Teesside University, Darlington DL11HG, United Kingdom*
[g] *School of Health & Life Sciences, Teesside University, Middlesbrough TS1 3BX, United Kingdom*
[h] *Department of Infectious Diseases, The Affiliated Hospital of Southwest Medical University, Luzhou 646000, China*

Received 16 April 2023; revised 22 June 2023; accepted 24 June 2023
Available online 7 July 2023

KEYWORDS

Non-fullerene Compounds;
DFT Study;
NLO Properties;
Frontier Molecular Orbitals;
Natural Bond Orbitals

Abstract In this work, non-fullerene based derivatives (**DTCD2-DTCD8**) with D1-π-D2-π-A architecture were tailored by alteration of terminal acceptor group of a reference molecule (**DTCR1**) in order to investigate their non-linear optical (NLO) behavior. The effect of peripheral acceptor and donor sites on designed configuration for optical communication and electronic response was examined using DFT based calculations. The natural bond orbitals (NBOs), frontier molecular orbitals (FMOs), UV–Vis analysis, nonlinear optics (NLO), density of states (DOS) and transition density matrix (TDM) were calculated at M06-2X/6-311G(d,p) level. The energy gap of **DTCD2-DTCD8** was found to be lowered (ΔE = 3.970–3.603 *eV*) with wider absorption spectra as compared to that of **DTCR1** (4.221 *eV*). All the derivatives (**DTCD2-DTCD8**) demonstrated significant

* Corresponding authors at: Institute of Chemistry, Khwaja Fareed University of Engineering & Information Technology, Rahim Yar Khan 64200, Pakistan (M. Khalid); Department of Infectious Diseases, The Affiliated Hospital of Southwest Medical University, Luzhou 646000, China (S.C. Ojha).
E-mail addresses: khalid@iq.usp.br (M. Khalid), suvash_ojha@swmu.edu.cn (S.C. Ojha).
Peer review under responsibility of King Saud University. Production and hosting by Elsevier.

Production and hosting by Elsevier

https://doi.org/10.1016/j.jscs.2023.101683

NLO behavior than the reference (**DTCR1**). Among all the designed compounds, **DTCD8** exhibited the highest dipole moment (μ_{total} = 4.777 *D*), average linear polarizability [$\langle\alpha\rangle$ = 1.920 × 10^{-22} *esu*], first hyperpolarizability (β_{total} = 10.58 × 10^{-28} *esu*) and second hyperpolarizability (γ_{total} = 8.028 × 10^{-33} *esu*) as it showed the lowest energy gap (3.603 *eV*) as compared to the other molecules.

1. Introduction

Now-a-days, NLO materials are considered to be one of the most significant materials due to their fascinating characteristics *i.e*., data transformation, fiber optics, photonic laser, data storage in the area of wireless communication and electro-optics [1]. Organic compounds possess large nonlinear properties, unique electronic and optic spectra and high structural flexibility when compared to inorganic compounds [2]. Organic molecules owing to their extended π-conjugated network can exhibit good photo thermal stability, molecular sensitivity, ease of molecular designing and rapid response time [3]. The organic compounds because of their non-centrosymmetric properties and push pull architecture consisting of π-spacer, electron-acceptor (A) and donor (D) moieties can be utilized to achieve fascinating $\langle\alpha\rangle$, β_{total} and γ_{total} values [4]. In such molecules, electrons transfer from donor to acceptor *via* π-conjugation give rise to an effective intermolecular charge transfer (ICT) creating a strong dipole moment and ultimately affecting their NLO properties [5]. The stability of lowest unoccupied molecular orbitals (LUMO) can be enhanced by the changing the position of electron withdrawing group (EWG) on the acceptor unit which also lowers the excitation energy and boosts the EW effect of acceptor units. The said parameters perform a very crucial role in establishing large NLO response [6]. The structural, electronic characteristics and E_{LUMO}-E_{HOMO} energy gaps efficiently tune the transfer of charge in organic systems [7]. The NLO properties of a compound can be improved through decreasing the ΔE of a molecule *via* increasing its conjugation [8]. There is an important role of 'D', 'A' and π-spacer configuration in reducing the band gap of organic compounds [9]. Hence, it is generally agreed that D-π-A configuration creates significant NLO responses as it has a strong push–pull framework which enhance the transference of electronic cloud in a molecule [10]. Literature is flooded with numerous efficient NLO materials with various push–pull configurations such as D-A, D-π-A, D-π-A-π-D, A-π-D-π-A, D-π-π-A, D-A-π-A and D-D-π-A [11]. Indeed, the type of substituents and extent of π-conjugation appreciably affect the NLO response of the materials [12]. In current era, NF based compounds have gained notable attention in photonic materials owing to the unique optical and electronic characteristics, easily tunable energy states, wide absorption spectra and reduced energy gap compounds [13,14]. The significant NLO behavior of NF chromophore is due to their (1) fully conjugated architecture, (2) isotropic electron-transfer rate, (3) electronegativity, (4) efficient electron delocalization between the electron rich (D) and electron deficient (A) regions [15]. Moreover, NFs consisting of planar structures and tunable energy gaps show appreciable stability as compared to the other organic systems [16]. NLO properties of NFs can also be improved by creating an appropriate π-conjugated system through the involvement of powerful 'D' and 'A' parts in NF molecules. For the donor system we selected carbazol moiety owing to its distinctive optoelectronic characteristics, varied energy gaps, high flexibility to structural modification makes it a suitable charge transporting material [17]. The presence of many alteration positions on carbazole makes it an interesting constituent for efficacious functional group integration where it can act as a core donor, peripheral donor and a π-bridge [18]. Thiophene ring is used as a π-linker to enhance the extended conjugation of the system and serves as a bridge to facilitate the movement of charge density in between donor and acceptor moieties [19]. Furthermore, addition of electronegative substituents (cyano and halogen groups) over the acceptor moieties of NFs scaffolding can also significantly affect the electronic characteristics of such molecules [20].

For this study, we have taken an efficient non-fullerene fused ring electron acceptor **DTCT-C-R** which exhibited the red-shifted absorption, lower excitation energies along with smaller energy gap (E_{gap} = E_{LUMO}-E_{HOMO}) and a sufficient power conversion efficiency (PCE) of 8.8%. According to best of our information, no literature is available regarding the NLO response of this molecule. Therefore, we designed seven compounds (**DTCD2-DTCD8**) by changing its architecture from A-π-D2-π-A to D1-π-D2-π-A and characterize their NLO response by density functional theory (DFT) and time dependent-DFT (TD-DFT) approaches. This might be the first detailed DFT study in order to elaborate NLO and electronic characteristics of **DTCT-C-R** based compounds. The prime goal of this research paper is to uncover potential remarkable dynamic materials with promising β_{total} and γ_{total} amplitudes. It is forecasted that our NLO-based investigation on these molecules would yield valuable results with the aim of achieving novel NFs NLO materials. These outcomes may open a new path for experimentalist to synthesize D–π–A framework-based modern fullerene-free organic compounds in order to get efficient NLO chromophores.

2. Computational detail

Gaussian 09 program package [21] was utilized for DFT calculations to explore NLO characteristics at M06-2X level [22] along with 6-311G(d,p) basis set [23] for **DTCR1** and **DTCD2-DTCD8**. FMOs [24], GRPs [25], TDM [26], DOS [27] and UV–Vis [28] analyses were performed with TD-DFT [29] calculations utilizing the aforesaid functional and basis set in dichloromethane (DCM) solvent. By the use of conductor-like polarizable continuum (CPCM) model [30] the solvent effect was investigated for absorption properties. For the evaluation of charge transfer interaction, NBOs was computed by

using 6.0 NBO package [31]. The input files of NF based studied compounds were generated by utilizing the GaussView 5.0 [32]. The true minima of entitled compounds at potential energy surface were developed by using the frequency analysis. Various softwares like Avogadro [33], Chemcraft [34], Origin 8.0 [35] and Multiwfn 3.7 [36] were used for the computation of results from output files. Along with M06-2X level, the dispersion corrected method: B3LYP-GD3BJ level of DFT [37] was studied to estimate the NLO characteristics of entitled chromophores. Dipole moment (μ), average linear polarizability $\langle a\rangle$, first hyperpolarizability (β_{total}) and second hyperpolarizability γ_{total} were determined by utilizing Eqs. (1)–(4) [36,38–41].

$$\mu = (\mu_x^2 + \mu_y^2 + \mu_z^2 2z)^{1/2} \quad (1)$$

$$\langle a\rangle = 1/3(\alpha_{xx} + \alpha_{yy} + \alpha_{zz}) \quad (2)$$

$$\beta_{\text{total}} = (\beta_x^2 + \beta_y^2 + \beta_z^2)^{1/2} \quad (3)$$

$$\gamma_{\text{total}} = \sqrt{\gamma_x^2 + \gamma_y^2 + \gamma_z^2} \quad (4)$$

where $\beta_x = \beta_{xxx} + \beta_{xyy} + \beta_{xzz}$, $\beta_y = \beta_{yyy} + \beta_{xxy} + \beta_{yzz}$, $\beta_z = \beta_{zzz} + \beta_{xxz} + \beta_{yyz}$ and $\gamma_i = \frac{1}{15}\sum_j(\gamma_{ijji} + \gamma_{ijij} + \gamma_{iijj})$ $i,j = \{x, y, z\}$.

3. Results and discussion

The current research is focused on comprehensive NLO studies of NF compounds (**DTCR1** and **DTCD2-DTCD8**) *via* DFT method. These compounds having D1-π-D2-π-A configuration consist of three fragments *i.e.*, 'D', 'A' and 'π-spacer' and their structural modification at terminal acceptor NLO properties are improved. The compound selected as reference 2-(5-{5-[7-[5-(4-diisocyanomethylene-6-oxo-4*H*,6*H*-cyclopenta[*c*]thiophen-5-ylidenemethyl)-thiophen-2-yl]-9-(1-octyl-nonyl)-9*H*-carbazol-2-yl]-thiophen-2-ylmethylene}-6-oxo-5,6-dihydro-cyclopenta[*c*]thiophen-4-ylidene)-malononitrile (**DTCT-C-R**) for current study, is already reported in literature with A-π-D-π-A configuration [42] consisting of hydrocarbon chain as *n*-octyl (-C_8H_{17}) group. The *n*-octyl group of parent molecule **DTC-T-C-R** is replaced with the methyl (—CH_3) group for the reduction of computational cost and to produce **DTCR1** (Fig. 1). Literature survey reveals that an efficient NLO response can be achieved by introducing powerful electron donating and accepting moieties at the terminals of a π-conjugated network [1]. Firstly, we designed **DTCD2** from the reference compound **DTCR1** *via* introduction of one 'D' 9-*H*-Carbazol and one π-linker thiophene prior to 'A' unit. Then **DTCD2** is utilized to model **DTCD3-DTCD8** molecules *via* tailoring terminal acceptor part as shown in Figs. 2 and 3. DFT computations are performed to calculate the absorption spectra, energies of LUMO-HOMO, transitions of NBOs, $\langle\alpha\rangle$, β_{total} and γ_{total}. It is expected that keen NLO response can be achieved from **DTCD2-DTCD8**. The chemical structures of the investigated molecules (**DTCR1** to **DTCD8**) are presented in Fig. 3. Additionally, the optimized structures are presented in Fig. S1 while cartesian coordinates are displayed in Tables S1–S8.

3.1. Electronic structure

The FMOs especially highest occupied molecular orbital (HOMO) and lowest unoccupied molecular orbital (LUMO) played a significant role in charge transferring and reactivity of a compound. Both of these MO levels are utilized to comprehend the electric reactivity and natural stability of the derivatives [43]. The electronic and optical properties of the molecules depend upon the electronic distribution in these HOMO and LUMO. The energy gap (E_{LUMO}-E_{HOMO}) reflects the tendency of a molecule to absorb light which is also associated with its molecular reactivity [44,45]. The small amplitude of energy gap results in high transfer of electronic cloud inside the molecule and improved NLO response [7]. Table 1 displays the HOMO, LUMO, HOMO-1, LUMO + 1, HOMO-2, LUMO + 2 energies and the energy gaps of the tailored compounds in DCM solvent.

The **DTCR1** possesses the energy gap of 4.221 *eV* along with the HOMO and LUMO energy values of −6.989 and −2.768 *eV*, respectively (Table 1). This Δ*E* was reduced to 3.603–3.970 *eV* in its derivatives (**DTCD2-DTCD8**) because of the change in configuration from A-π-D-π-A to D1-π-D2-π-A. The reduction of Δ*E* to 3.970 *eV* in **DTCD2** could be due to the introduction of one 'D' 9*H*-carbazole and one π-spacer moiety thiophene, which resulted in enhanced conjugation and powerful push–pull architecture. This Δ*E* was further decreased to 3.931 and 3.934 *eV* in **DTCD3** and **DTCD4**, respectively owing to the existence of one/two powerful electronegative fluoro groups as 2-(5-Fluoro-2-methylene-3-oxo-indan-1-ylidene)-malononitrile (**DTCD3**) and 2-(5,6-Difluoro-3-oxo-indan-1-ylidene)-malononitrile (**DTCD4**) at the 'A' site. In case of resonance, chloro (-Cl) group promotes the transference of its non-bonded electronic pair towards acceptor moieties. Therefore, a slight increase 3.938 *eV* in LUMO-HOMO energy gap was noticed for the compound **DTCD5** in which only one chloro group is present on the electron accepting unit as 2-(5-Chloro-2-methylene-3-oxo-indan-1-ylidene)-malononitrile. This enhancement in energy gap might be owed to the electron resonating effect of -Cl moiety. A remarkable reduction in the Δ*E* to 3.803 *eV* was observed in

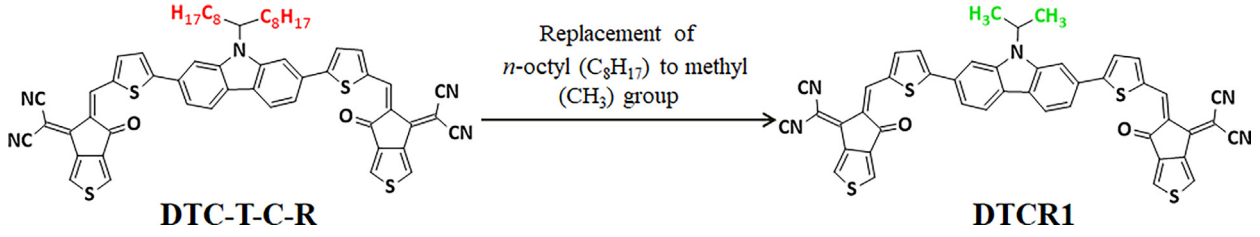

Fig. 1 Modification of **DTC-T-C-R** [71] into **DTCR1***via* substitution of small alkyl group.

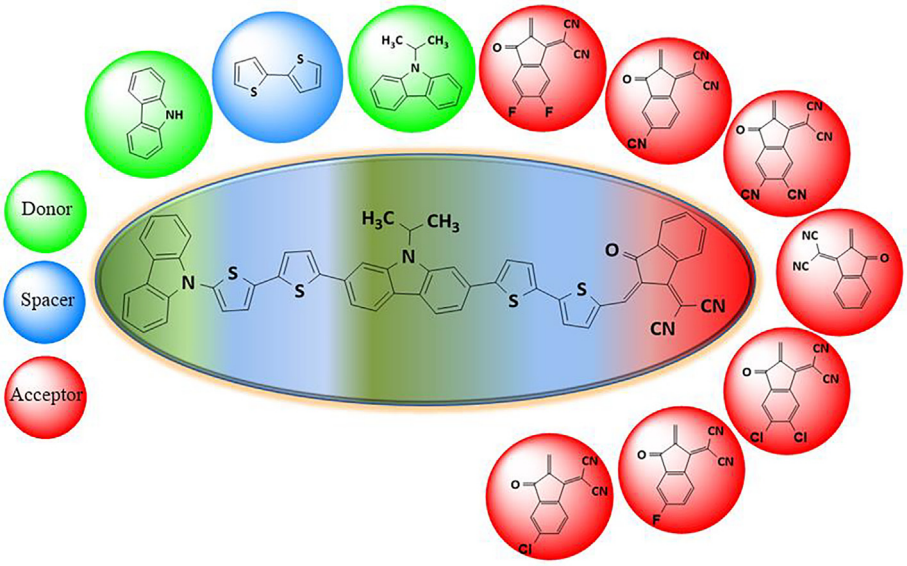

Fig. 2 The outline map of designed compounds (**DTCD2-DTCD8**) *via* reference compound.

DTCD6 as two fluoro groups of the 'A' moiety were exchanged with two chloro groups in the form of 2-(5,6-Dichloro-3-oxo-indan-1-ylidene)-malononitrile. The chloro groups at the 'A' position of **DTCD6** express lower inductive (*I*) effect as compared to the fluoro groups at the same position, resulting in the less transfer of electrons. Also, chloro group exhibits more electron donating resonance effect as compared to fluoro group (Cl > F) [46]. Thus, a decline in the energy gap of **DTCD6** was reported due to the less (*I*) effect and higher resonance effect caused by the chloro-groups. Further, decrease in energy gap (3.726 *eV*) in **DTCD7** as compared to that (3.603 *eV*) of **DTCD8** was recorded due to the existence of only one (—CN) at the 'A' site as 2-(5-Isocyano-3-oxo-indan-1-yli dene)-malononitrile. The lowest E_{LUMO}-E_{HOMO} energy gap 3.603 *eV* in **DTCD8** was noted due to the introduction of two —CN groups at the 'A' part as 2-(6-Cyano-5-isocyano-3-oxo-indan-1-ylidene)-malononitrile; it was due to higher inductive effect of —CN in comparison to —F and —Cl. Moreover, because of the great EW potential of —CN groups the chances of charge transfer were increased, resulting in lower energy gap. Table 1 discloses that energy trend of HOMO-1, HOMO-2, LUMO + 1, LUMO + 2 and their corresponding energy gaps is almost similar to LUMO-HOMO in all the investigated compounds (**DTCR1** and **DTCD2-DTCD8**). Overall LUMO-HOMO, LUMO + 1-HOMO-1, LUMO + 2-HOMO-2 energy gap has the following decreasing trend: **DTCR1 > DTCD2 > DTCD5 > DTCD4 > DTCD3 > DTC D6 > DTCD7 > DTCD8**. Hence, the shift of electronic charge to the acceptor moiety was significantly enhanced by introduction of EWG's at the acceptor site of a precursor; this charge shift results in lower value of energy gap and enhanced NLO behavior.

The energy gap magnitude characterizes the migration of ICT from donor to acceptor portion through π-spacer, and provides insights about NLO behavior. The surface areas of FMOs were utilized to determine the charge transference, as presented in Figs. S2–S9. In reference molecule (**DTCR1**), the electronic cloud for HOMO was located on to the central 'D' (9-Isopropyl-2,7-di-thiophen-2-yl-9*H*-carbazole) and π-spacer (thiophene), whereas for LUMO, the significant part of charge density was concentrated on the 'A' moiety *i.e.,* 2-(6-Oxo-5,6-dihydro-cyclopenta[*c*]thiophen-4-ylidene)-malono nitrile. In **DTCD2-DTCD8**, the charge density for HOMO primarily exists on 9*H*-Carbazole 'D' whereas, a little amount of charge density was also located on to the first π-spacer. LUMO was lying slightly on second π-linker and dominantly on 'A' unit. Hence, there was a remarkable transfer of electronic charge in the investigated molecules from 'D' to 'A' with the aid of π-spacer moiety. This rise of charge transfer validates that all the analyzed molecules may find future applications as efficient NLO materials. The pictorial demonstration of HOMO−1, LUMO + 1, HOMO−2, and LUMO + 2 is manifested in Figs. S10–S25.

3.2. Global reactivity parameters (GRPs)

The (ΔE = LUMO–HOMO) is helpful in the estimation of global reactivity descriptors (GRDs) as used to explore the dynamic stability and chemical reactivity of molecules. The molecules having larger energy difference between HOMO and LUMO are suggested as harder molecules with more stability, less reactivity and vice versa [25]. Compound's ability to loose or gain electron is measured from the electron affinity and ionization potential values, whereas electronegativity gives the indication about its reactivity as it is the tendency of a compound to pull the electrons towards itself. Similarly, electrophilicity index lists the tendency of compounds to accept electrons and is determined by employing the chemical hardness and chemical potential [$\omega = \mu^2/2\eta$] [47]. The parameters *i.e.*, electron affinity (*EA*), global hardness (η), electronegativity (X), ionization potential (*IP*), global softness (σ), global electrophilicity (ω) and chemical potential (μ) were computed by using Eqs. (S1)–(S7) (cited in SI);the obtained data is given in Table 2.

Table 2 shows significantly high values of '*EA*' of designed compounds except DTCD2, DTCD3 and DTCD5 as compared to DTCR1 due to the existence of strong 'A' units. In

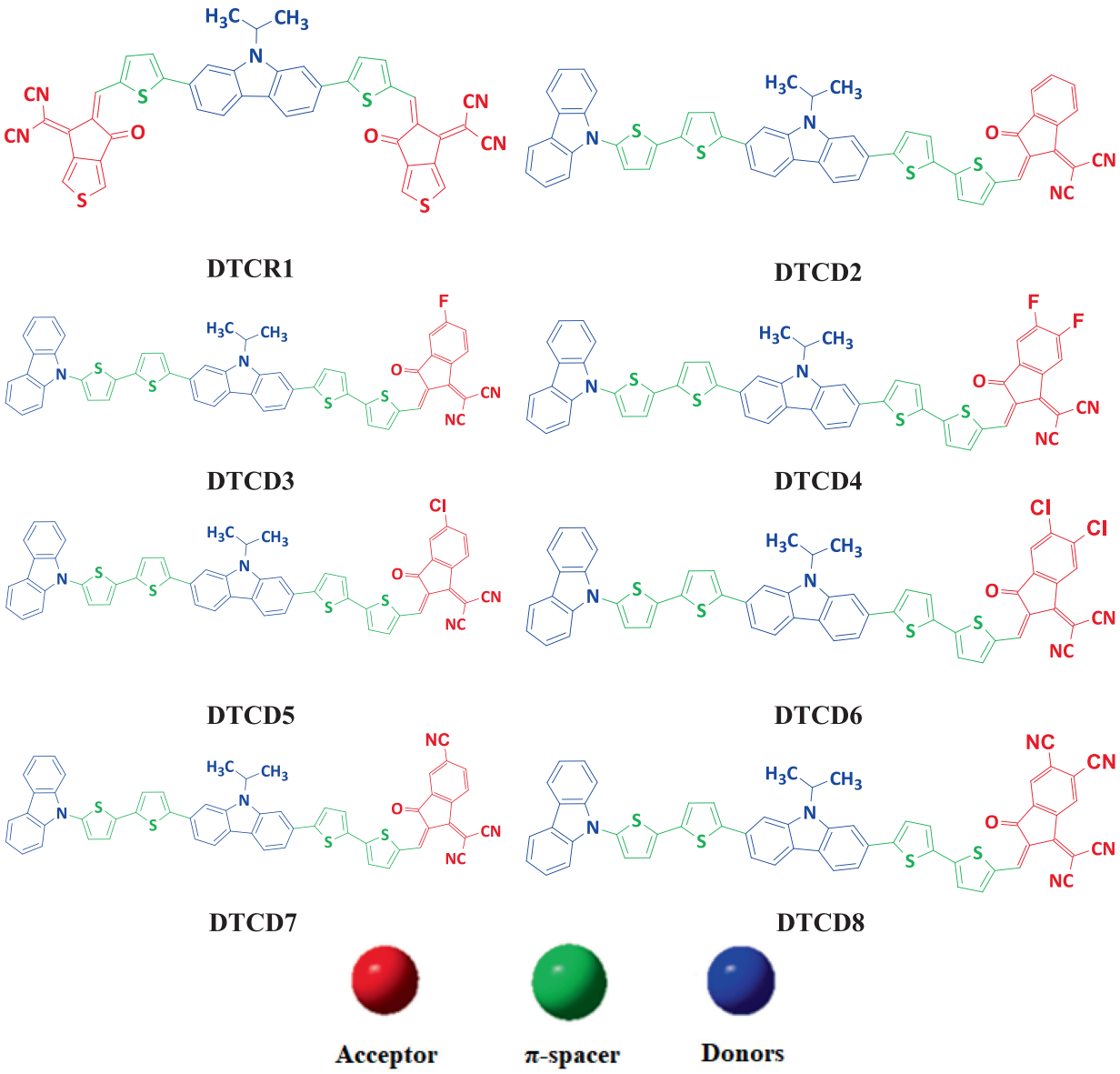

Fig. 3 The chemical structures of reference (**DTCR1**) and designed compounds (**DTCD2-DTCD8**).

Table 1 E_{HOMO}, E_{LUMO}, E_{HOMO-1}, E_{LUMO+1}, E_{HOMO-2}, E_{LUMO+2} and energy gap (E_{LUMO}-E_{HOMO}) of studied compounds.

Compounds	DTCR1	DTCD2	DTCD3	DTCD4	DTCD5	DTCD6	DTCD7	DTCD8
HOMO	−6.989	−6.688	−6.668	−6.731	−6.726	−6.689	−6.680	−6.709
LUMO	−2.768	−2.718	−2.737	−2.797	−2.788	−2.866	−2.954	−3.106
Energy Gap	4.221	3.970	3.931	3.934	3.938	3.823	3.726	3.603
HOMO-1	−7.274	−7.064	−7.019	−7.121	−7.112	−7.066	−7.031	−7.093
LUMO + 1	−2.640	−1.887	−1.968	−2.000	−2.016	−2.106	−2.167	−2.608
Energy Gap	4.634	5.177	5.051	5.121	5.096	4.960	4.864	4.485
HOMO-2	−7.611	−7.181	−7.184	−7.191	−7.188	−7.190	−7.193	−7.205
LUMO + 2	−1.540	−1.283	−1.308	−1.298	−1.297	−1.343	−1.334	−1.457
Energy Gap	6.071	5.898	5.876	5.893	5.891	5.847	5.859	5.748

Units in *eV*.

our designed chromophores (**DTCD2-DTCD8**) the '*IP*' values (0.245–0.247 E_h) were lower than the reference chromophore (0.257 E_h) which expressed facile removal of electrons and lesser energy needed to make them polarized than DTCR1. All the derivatives exhibited higher values of 'η' with smaller 'σ' values which demonstrate that designed chromophores were

Table 2 Global reactivity descriptor of **DTCR1** and **DTCD2-DTCD8.**

Parameters	DTCR1	DTCD2	DTCD3	DTCD4	DTCD5	DTCD6	DTCD7	DTCD8
IP	0.257	0.246	0.245	0.247	0.247	0.246	0.245	0.247
EA	0.102	0.100	0.101	0.103	0.102	0.105	0.109	0.114
X	0.179	0.173	0.173	0.175	0.175	0.176	0.177	0.180
η	0.078	0.073	0.072	0.072	0.072	0.070	0.068	0.066
μ	−0.179	−0.173	−0.173	−0.175	−0.175	−0.176	−0.177	−0.180
ω	0.207	0.205	0.207	0.212	0.211	0.219	0.229	0.246
σ	0.009	0.009	0.009	0.009	0.009	0.010	0.010	0.010

Units in *Hatree* (E_h).

chemically stable and less reactive. Descending trend of 'σ' was **DTCD8 = DTCD7 = DTCD6 > DTCD5 = DTCD4 = D TCD3 = DTCD2 = DTCR1** with the values of 0.010 > 0.010 > 0.010 > 0.009 = 0.009 = 0.009 = 0.009 = 0.009 E_h, respectively (Table 2). Furthermore, the larger 'ω' values (0.246–0.205 E_h) along with greater 'η' values demonstrate high ability of a molecule to pull out electrons and serve as an electrophile. The effect of acceptor moieties in calculating the values of 'μ' was more negative (−0.180 to −0.173 E_h) which progressively makes the molecules greatly polarizable chemically more reactive and kinetically least stable as displayed in the above-mentioned compounds. From this discussion, it was concluded that higher charge shifting tendency of molecules among their LUMO and HOMO orbitals give rise to enhanced polarizability and auspicious NLO behavior.

3.3. Natural Bond Orbitals (NBOs) study

NBOs analysis explains the charge transfer in D-π-A schemes *via* interpretation of conjugative interactions and gives understanding of second order stabilization energy associated with filled and empty orbitals of the compounds [48]. Eq. (5) was employed to determine the second order stabilization energy [49].

$$E^{(2)} = q_i \frac{(F_{i,j})^2}{(E_j - E_i)} \tag{5}$$

where $E^{(2)}$ is the stabilization energy, E_j and E_i are diagonal element orbital energies, q_i is the donor-orbital occupancy and $F_{i,j}$ is the Fock matrix element between the NBOs [49]. In this analysis, the assessment of higher E^2 amplitude demonstrates that there was a significant interaction between Lewis (D), non-Lewis (A) orbitals and conjugation was appeared which results in stability of the molecule [50]. Table 4 shows few exemplary interactions while bunch of other electronic transitions was displayed in Tables S9–S16.

Table 3 NBOs charges for donor, π-spacer, and acceptor moieties of **DTCR1** and **DTCD2–DTCD8.**

Compounds	Donor	π-Spacer	Acceptor
DTCR1	0.282321	−0.020861	−0.26146
DTCD2	0.360981	0.097062	−0.13054
DTCD3	0.029267	0.112215	−0.141477
DTCD4	0.03674	0.108308	−0.14504
DTCD5	0.036649	0.108182	−0.144829
DTCD6	0.034137	0.120248	−0.15439
DTCD7	0.033553	0.132078	−0.165626
DTCD8	0.039613	0.151147	−0.19076

Table 3 shows the NBO charges that were calculated for donor, π-linker and acceptor moieties. The positive charge on 'D' and π-bridge section in all molecules indicated the transfer of proficient electronic charge towards the negatively charged acceptor 'A' unit. The positively charged π-conjugated linkers cannot entrap the electrons and facilitate the electronic pathway to acceptors.

Table 4 mentions four important types of transitions *i.e.*, π → π*, σ → σ*, LP → π* and LP → σ*. The most dominant transitions were π → π* which occur because of π-conjugation in the studied compounds. The σ → σ* electronic transitions were weak electronic transitions as compared to all other types. In **DTCR1**, the most probable π → π* electronic transitions were found as π(C40-C42) → π*(C44-C45) with 34.13 *kcal/mol* stabilization energy, whereas the remaining seven compounds **DTCD2-DTCD8** exhibit the highest stabilization energy values of 34.41, 35.20, 35.53, 53.46, 36.12, 36.85 and 38.71 *kcal/mol* for π(C75-C77) → π*(C79-C81) electronic transitions. The least probable transitions of same type were π(C68-N69) → π*(C66-N67), π(C88-N89) → π*(C86-N 87), π(C86-N87) → π*(C88-N89), π(C86-N87) → π*(C88-N8 9), π(C88-N89) → π*(C86-N87), π(C86-N87) → π*(C88-N89), π(C86-N87) → π*(C88-N89) and π(C86-N87) → π*(C88-N89) with very little stabilization energy values 0.64, 0.83, 0.81, 0.79, 0.82, 0.78, 0.80 and 0.78 *kcal/mol*, respectively. The highest 10.45, 10.58, 10.65, 10.63, 10.62, 10.64, 10.75 and 10.82 *kcal/mol* stabilization energy in **DTCR1** and **DTCD2-DTCD8** correspond to σ(C44-H46) → σ*(S39-C42) (**DTCR1**) σ(C79-H80) → σ*(S74-C77) (**DTCD2-DTCD8**) electronic transitions. As σ → σ* transitions with the lowest 0.50, 0.50, 0.51, 0.51, 0.50, 0.50, 0.50 and 0.51 *kcal/mol* stabilization energy values for σ → σ* transitions have noted in σ(C73-S 75) → σ*(C55-C57), σ(C22-H25) → σ*(C20-H21), σ(C75-H 77) → σ*(C35-H72), σ(C75-H77) → σ*(C35-H72), σ(C22-H 25) → σ*(C20-H21), σ(C26-H28) → σ*(N19-C20), σ(C75-H 77) → σ*(C79-H80) and σ(C75-H77) → σ*(C79-H80) electronic transitions for **DTCR1** and **DTCD2-DTCD8**, respectively. The lone pair transitions have also shown some important amplitudes of stability *i.e.*, 49.38, 48.95, 48.91, 48.92, 48.94, 48.90, 48.91 and 48.77 *kcal/mol* observed in LP1(N19) → π*(C14-C15) (**DTCR1** and **DTCD2-DTCD7**) and LP1(N19) → π*(C3-C4) (**DTCD8**), whereas 0.51, 0.52, 0.53, 0.52, 0.52, 0.51, 0.53 and 0.51 *kcal/mol* noted in electronic transitions LP1(N19) → σ*(C26-H29) (**DTCR1** and **DTCD2-DTCD8**), respectively.

From the above analysis, it was clarified that **DTCD8** shows higher NBOs value as compared to all other designed

Table 4 Remarkable NBO interactions for entitled compounds.

Compounds	Donor(*i*)	Type	Acceptor(*j*)	Type	*E*(2) (*kcal/mol*)	*E(j)-E(i)*[b] (*a.u*)	*F(I,j)*[c](*a.u*)
DTCR1	C40—C42	π	C44—C45	π*	34.13	0.38	0.103
	C68—N69	π	C66—N67	π*	0.64	0.58	0.017
	C44—H46	σ	S39—C42	σ*	10.45	0.85	0.084
	C73—S75	σ	C55—C57	σ*	0.50	1.27	0.023
	N19	LP(1)	C14—C15	π*	49.38	0.35	0.121
	N19	LP(1)	C26—H29	σ*	0.51	0.78	0.020
DTCD2	C75—C77	π	C79—C81	π*	34.41	0.38	0.104
	C88—N89	π	C86—N87	π*	0.83	0.57	0.019
	C79—H80	σ	S74—C77	σ*	10.58	0.85	0.085
	C22—H25	σ	C20—H21	σ*	0.50	1.06	0.021
	N19	LP(1)	C14—C15	π*	48.95	0.35	0.121
	N19	LP(1)	C26—H29	σ*	0.52	0.78	0.020
DTCD3	C75—C77	π	C79—C81	π*	35.20	0.38	0.105
	C86—N87	π	C88—N89	π*	0.81	0.58	0.019
	C79—H80	σ	S74—C77	σ*	10.65	0.85	0.085
	C75—C77	σ	C35—C72	σ*	0.51	1.36	0.024
	N19	LP(1)	C14—C15	π*	48.91	0.35	0.121
	N19	LP(1)	C26—H29	σ*	0.53	0.78	0.020
DTCD4	C75—C77	π	C79—C81	π*	35.53	0.38	0.105
	C86—N87	π	C88—N89	π*	0.79	0.58	0.019
	C79—H80	σ	S74—C77	σ*	10.63	0.85	0.085
	C75—C77	σ	C35—C72	σ*	0.51	1.36	0.024
	N19	LP(1)	C14—C15	π*	48.92	0.35	0.121
	N19	LP(1)	C26—H29	σ*	0.52	0.78	0.020
DTCD5	C75—C77	π	C79—C81	π*	35.46	0.38	0.105
	C88—N89	π	C86—N87	π*	0.82	0.57	0.019
	C79—H80	σ	S74—C77	σ*	10.62	0.85	0.085
	C22—H25	σ	C20—H21	σ*	0.50	1.06	0.021
	N19	LP(1)	C14—C15	π*	48.94	0.35	0.121
	N19	LP(1)	C26—H29	σ*	0.52	0.78	0.020
DTCD6	C75—C77	π	C79—C81	π*	36.12	36.12	0.38
	C86—N87	π	C88—N89	π*	0.78	0.78	0.58
	C79—H80	σ	S74—C77	σ*	10.64	10.64	0.85
	C26—H28	σ	N19—C20	σ*	0.50	0.50	0.97
	N19	LP(1)	C14—C15	π*	48.90	48.90	0.35
	N19	LP(1)	C26—H29	σ*	0.51	0.51	0.78
DTCD7	C75—C77	π	C79—C81	π*	36.85	0.38	0.106
	C86—N87	π	C88—N89	π*	0.80	0.58	0.019
	C79—H80	σ	S74—C77	σ*	10.75	0.85	0.085
	C75—C77	σ	C79—H80	σ*	0.50	1.30	0.023
	N19	LP(1)	C14—C15	π*	48.91	0.35	0.121
	N19	LP(1)	C26—H29	σ*	0.53	0.78	0.020
DTCD8	C75—C77	π	C79—C81	π*	38.71	0.37	0.108
	C86—N87	π	C88—N89	π*	0.78	0.58	0.019
	C79—H80	σ	S74—C77	σ*	10.82	0.85	0.086
	C75—C77	σ	C79—H80	σ*	0.51	1.30	0.023
	N19	LP(1)	C3—C4	π*	48.77	0.19	0.128
	N19	LP(1)	C26—H29	σ*	0.51	0.78	0.020

molecules and it may play an important role as one of the efficient NLO materials in the current research.

3.4. Absorption analysis

The basic principle of UV–Vis spectra is electronic transition from ground level to the first excited level because of absorption of electrons which was employed to evaluate the optical characteristics [28] of our investigated molecules by TD-DFT computations in DCM solvent and gaseous phase. Few notable transitions of investigated compounds (**DTCR1** and **DTCD2-DTCD8**) were displayed in Table 5, whereas other electronic transitions were represented in Tables S17–S32 and their UV–Vis spectra were shown in Figs. 4, S26 and S27. The electronic transition from π-bonding molecular orbital *i.e.*, HOMO to π* anti-binding molecular orbital *i.e.*, LUMO correlates to absorption of electrons [51] and extended conjugation along with strong terminal EWG shows larger red shift in UV–Vis absorption spectra. The investigated molecules with D1-π-D2-π-A configuration having acceptors with numerous electronegative substituents show different optoelectronic characteristics.

Table 5 Wavelength (λ), excitation energy (E), oscillator strength (f_{os}) and nature of molecular orbital contributions of entitled molecules in DCM solvent and Gaseous phase.

Medium	Compounds	$\lambda(nm)$	$E\ (eV)$	f_{os}	MO contributions
Dichloromethane	**DTCR1**	468.640	2.646	3.045	H → L(71%)
	DTCD2	485.125	2.556	1.997	H-1 → L(28%),H → L(50%)
	DTCD3	485.771	2.552	2.009	H-1 → L(38%),H → L(38%)
	DTCD4	488.566	2.538	1.931	H-1 → L(26%),H → L(48%)
	DTCD5	490.673	2.527	1.960	H-1 → L(26%),H → L(49%)
	DTCD6	500.114	2.479	2.001	H-1 → L(33%),H → L(42%)
	DTCD7	511.525	2.424	1.912	H-1 → L(36%),H → L(39%)
	DTCD8	524.043	2.366	1.914	H-1 → L(31%),H → L(38%)
Gaseous Phase	**DTCR1**	434.755	2.852	0.411	H-4 → L(18%),H-6 → L(2%)
	DTCD2	462.021	2.684	2.007	H-1 → L(24%),H → L(47%)
	DTCD3	463.385	2.676	2.023	H → L(32%),H-1 → L(38%)
	DTCD4	466.313	2.659	1.929	H-2 → L(21%),H → L(43%)
	DTCD5	467.368	2.653	1.965	H-2 → L(20%),H → L(45%)
	DTCD6	476.053	2.604	2.011	H-1 → L(28%),H → L(36%)
	DTCD7	487.394	2.544	1.903	H → L(30%),H-1 → L(36%)
	DTCD8	500.660	2.476	1.890	H-1 → L(23%),H → L(31%)

MO = molecular orbital, H = HOMO, L = LUMO, f_{os} = oscillator strength.

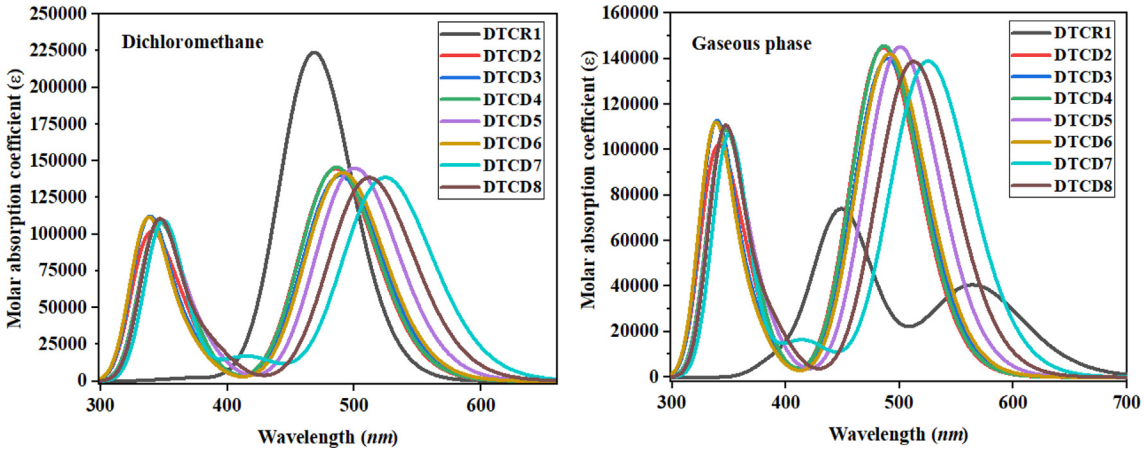

Fig. 4 Simulated absorption spectra of investigated compounds (**DTCR1** and **DTCD2-DTCD8**).

Table 5 shows that **DTCR1** have simulated λ_{max} at 468.640 (in DCM) and 434.755 *nm* (in gas phase) with excitation energy values of 2.646 and 2.852 *eV*, respectively. There was a significant red-shift in **DTCD2-DTCD8** as compared to **DTCR1** in DCM as well as in gaseous phase. Also absorption occurred at higher λ_{max} (bathochromic shift) in DCM (485.125–524.043 *nm*) with excitation energy (2.366–2.556 *eV*) as compared to that (462.021–500.660 *nm*) with (2.476–2.684 *eV*) in the gaseous phase (Fig. 4) in these compounds (**DTCD2-DTCD8**); it is due to the interconnection of EWGs on 'A' units with DCM solvent. This interaction has lowered the ΔE between the ground and excited levels and resulted in bathochromic shift and outstanding optical characteristics. Among **DTCD2-DTCD8**, the **DTCD8** has displayed highest λ_{max} values in DCM (524.043 *nm*) as well as in gaseous phase (500.660 *nm*) with the excitation energies of 2.366 and 2.476 *eV*, respectively; it is due to the very strong negative inductive (–I) effect of ⎓CN groups in **DTCD8**. The lowest absorbance (485.125 *nm* in DCM and 462.021 *nm* in gas phase) was observed for **DTCD2** with the excitation energy values of 2.556 and 2.684 *eV*, correspondingly. The λ_{max} was decreased in the same order in DCM solvent as well as in gas phase: **DTCD8 > DTCD7 > DTCD6 > DTCD5 > DTCD4 > DTCD3 > DTCD2 > DTCR1.** It is worth mentioning that the electronic absorption spectra of **DTCD2-DTCD8** lied in visible region in gaseous phase as well as in DCM solvent (Table 5).

3.5. Transition Density Matrix (TDM) and Exciton-Binding Energy (E_b)

TDM computations were done for the complete understanding of transition behavior from S0 to S1 state [26,52]. This analysis with the help of three-dimensional plots, effectively elaborates the (1) movement of electronic charge density from 'D' to 'A' entities *via* π-conjugation in excited state, (2) charge excitation phenomena and (3) localization and delocalization of electron hole pairs [26,53]. In this analysis, efficacy of hydrogen (H) atoms has been ignored by default due to their insignificant

role in electronic transitions. TDM plot of all the entitled molecules determines the kind of electronic transition in these molecules. TDM outcomes of all the studied molecules were presented in Fig. 5. To acknowledge the transfer of electronic cloud we categorize all the structures (**DTCR1** and **DTCD2-DTCD8**) into three segments ('D', 'A' and π-linkers) to simplify the calculations. TDM pictographs displayed an effective diagonal charge transfer (CT) in all the afore-mentioned compounds. In **DTCR1** the greater electronic charge can be perceived on 'D' and π-spacer and little amount of it was seen on 'A' of the TDM plots as demonstrated by green and red spots. In **DTCD2-DTCD8** the marvelous charge density was

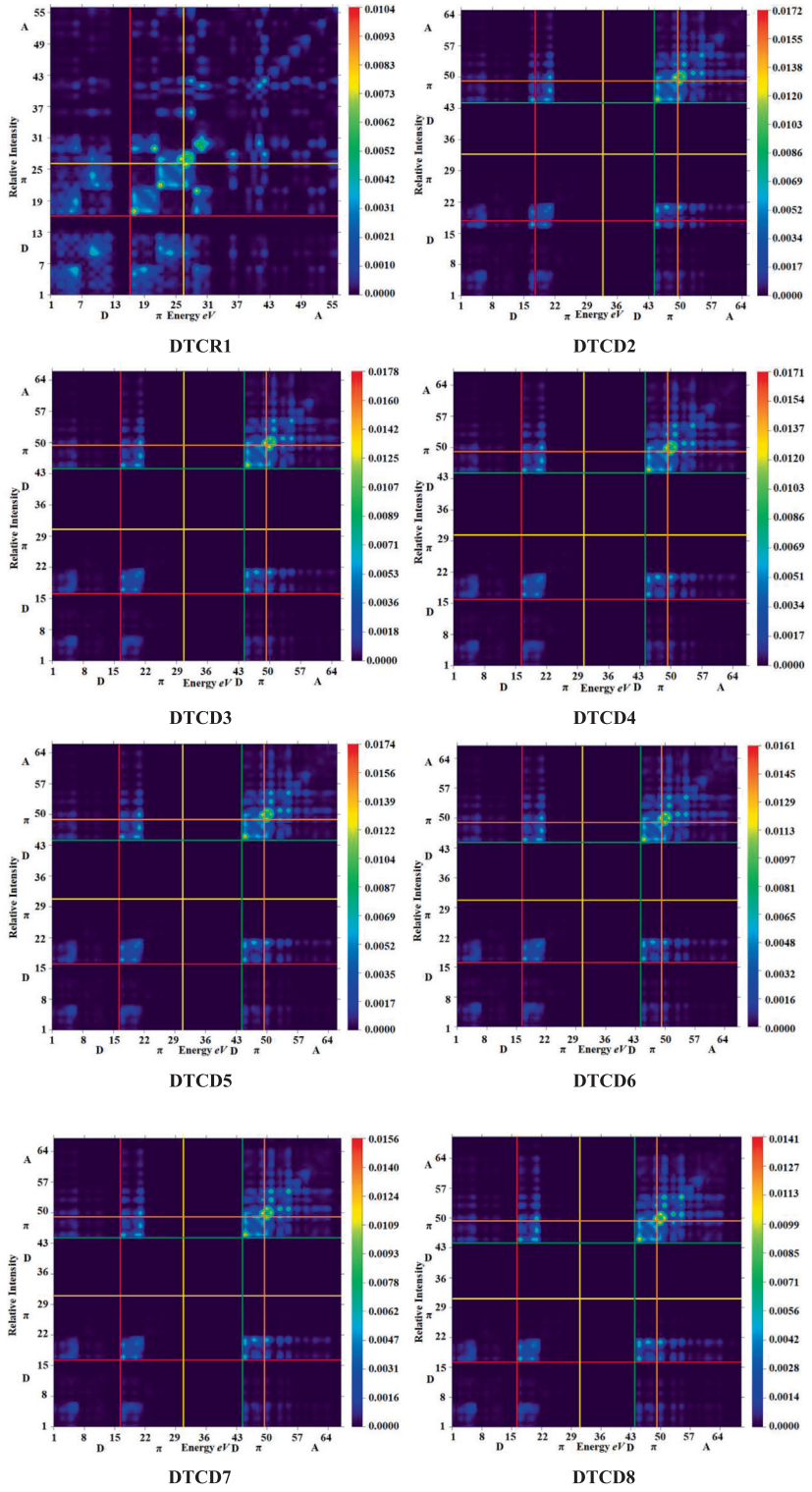

Fig. 5 Transition density matrix (TDM) heat maps of **DTCD2-DTCD8** and **DTCR1** compounds at S_1 state.

observed at the donor and acceptor parts however, little electronic cloud was examined on π-spacer which manifests that electrons were proficiently shifted from donor to π-linker, which superiorly promotes the transfer of electronic charge density towards 'A' without any hindrance (Fig. 5). This exclusive behavior might be because of the existence of highly EWG (—CN and —F) on the 'A' moiety. The results of TDM plots signify simple and larger exciton dissociation in the excited level, which is extremely significant for the development of NLO materials.

Another major tool for prediction of ICT of different materials is the binding energy (E_b). Low binding energy leads to higher charge mobilities and greater NLO response. The exciton binding energies of **DTCD2-DTCD8** and **DTCR1** were determined by subtracting the ΔE from first excitation energy values. E_b was calculated by using Eq. (6).

$$E_b = E_{L-H} - E_{opt} \tag{6}$$

In Eq. (6), $E_{L\text{-}H}$ is the energy gap between HOMO and LUMO and E_{opt} is the first excitation energy obtained from S_0 to S_1 [52]. The theoretical calculations of E_b were shown in the Table 6.

It was quite enchanting that all the derivatives (**DTCD2-DTCD8**) exhibit lower E_b amplitudes (1.237–1.411 *eV*) in contrast to the reference (**DTCR1**) (1.575 *eV*). These lower E_b values may be because of the change in framework, which generates a powerful push–pull mechanism. Similarly, excitation energies of DTCD2-DTCD8 were smaller than those of DTCR1 with the same order of the ΔE = LUMO-HOMO. This smaller E_b with lower excitation energy value and energy gap facilitates the greater excitation dissociation and excellently higher charge density flow with enhanced optoelectronic properties. The binding energies of the studied compounds were descended in the following trend: **DTCR1 > DTCD3 > DTCD7 > DTCD2 > DTCD5 > DTCD4 > DTCD8 > DTCD6** which is noted to be in good harmony with the TDM study. Small binding energies possess a direct correlation with polarizability and compounds having 1.9 *eV* binding energy value are regarded as ideal photonic materials. Attractively, all our designed chromophores manifested E_b smaller than 1.9 *eV* have great charge dissociation in excited levels representing them to be remarkable NLO compounds.

3.6. Density of States (DOS)

In order to systematically recognize the structure-NLO character correlation of investigated molecules the precise offering of an individual portion in the form of DOS has been estimated by utilizing PyMOlyze 2.0 software at the abovementioned level [27,35]. DOS investigation was utilized to support results of studied compounds (**DTCR1** and **DTCD2-DTCD8**) displayed in FMOs diagrams (Figs. S2–S9). By altering the terminal 'A' units, the electronic cloud scattering was migrated in distinct arrangements around LUMO and HOMO orbitals as can be seen in DOS graphs. DOS displays the type of all associating groups (that are exist in a compound) with charge transference from HOMO to LUMO of the compound [27,54]. To explain the DOS study, each compound was divided into four segments, *i.e.,* 'D1' 9*H*-carbazole, π-spacer thiophene, 'D2' Ethylidene-1-isopropyl-2,3-dihydro-1*H*-indole and 'A' 2-(2-Methylene-3-oxo-indan-1-ylidene)-malononitrile; they were depicted through red, green, blue and pink lines, respectively in the DOS spectra. From Fig. 6 it was permitted that the charge density of HOMO in the **DTCR1** was only concentrated on the central 'D' and π-core, whereas the LUMO electronic cloud was focused on the 'A' part. In **DTCD2-DTCD8** a comparable charge distribution framework of LUMO/HOMO density was examined such as maximum portion in the 'A' and minimum portion over the π-spacer. The electronic and photovoltaic properties of derivatives **DTCD2-DTCD8** were significantly enhanced due to strong movement of the electron densities as proved by the distribution patterns of LUMO/HOMO. For the reference molecule (DTCR1), the greatest electronic cloud of HOMO was noted to be −7.5 *eV*, and it was concentrated on the 'D' moiety, whereas the greatest electronic cloud for LUMO was observed to be 2 to 3 *eV* by the 'A' part and little contribution was also seen by the π-linker. For the designed compounds (**DTCD2-DTCD8**) the greatest electronic cloud of HOMO was noticed to be −7.1 and −7.2 *eV*, and it was concentrated on 'D1' and 'D2' moieties, whereas the greatest electronic cloud for LUMO was noted to be 2.8 to 3 *eV* by the 'A' part and slight contribution was also perceive by the π-spacer. In **DTCR1** 'D' contribution was found to be 49.2% to HOMO and 7.7% to LUMO, whereas 'A' and π-spacer contributes 19.2 and 31.6% to HOMO and 70.1 and 22.1% to LUMO. These contributions were altered efficiently in fabricated compounds because of the use of various EWG on 'A' unit. For 'D1' the electronic contribution on HOMO was observed to be 3.5, 8.2, 2.1, 2.1, 5.0, 8.0 and 5.7% while on LUMO was examined to be 0.0, 0.0, 0.0, 0.0, 0.0, 0.0, and 0.0%, respectively in **DTCD2-DTCD8**. Similarly, electronic cloud contribution for π-spacer was noted to be 54.3, 54.8, 54.3, 54.3, 55, 54.6 and 54.9% on HOMO, whereas it was found to be 45.4, 47.5, 44.5, 45, 43.6, 39.3 and 34.4% for LUMO in **DTCD2-DTCD8**, respectively. It was also cleared that 'D2' at HOMO contributes 37.4, 33.8, 39.1, 38.7, 36.2, 33.9 and 36 % whereas its contribution was found to be 1.6, 1.5, 1.2, 1.3, 1.4, 1.2 and 1% at LUMO for **DTCD2-DTCD8**, respectively. 'A' has shown 4.8, 3.2, 4.5, 4.9, 3.7, 3.5 and 3.3% contribution at HOMO while it was found to be 53, 51.1, 54.2, 53.7, 55, 59.6 and 64.6% at LUMO for **DTCD2-DTCD8**, respectively. In **DTCD8** the

Table 6 Calculated LUMO-HOMO energy gap ($E_{LUMO\text{-}HOMO}$), first singlet excitation energy (E_{opt}) and exciton binding energy (E_b).

Compounds	DTCR1	DTCD2	DTCD3	DTCD4	DTCD5	DTCD6	DTCD7	DTCD8
$E_{L\text{-}H}$	4.221	3.970	3.931	3.934	3.938	3.803	3.726	3.603
E_{opt}	2.646	2.556	2.552	2.538	2.527	2.479	2.424	2.366
E_b	1.575	1.396	1.414	1.324	1.379	1.237	1.411	1.302

Units in *eV*.

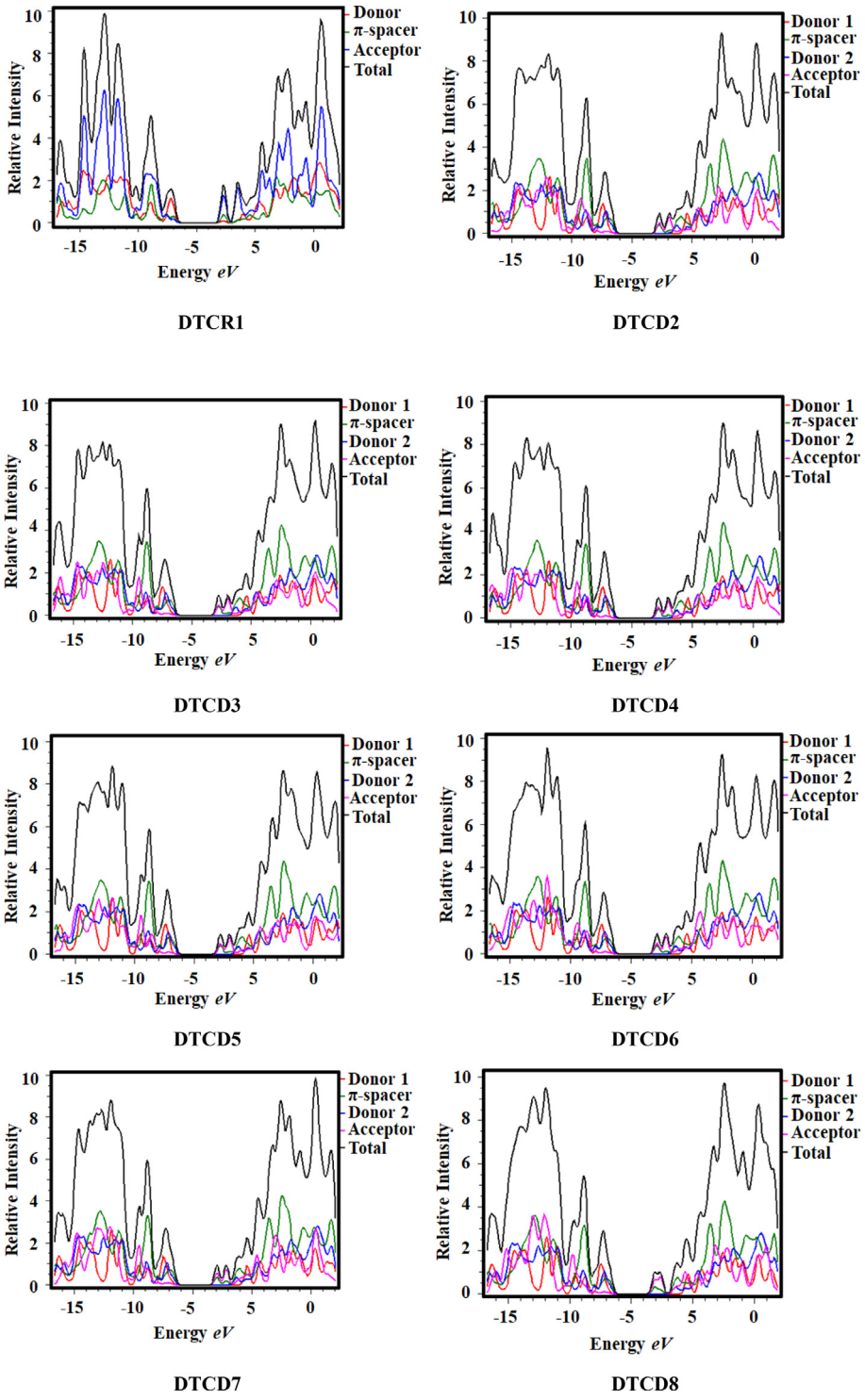

Fig. 6 DOS plots of reference **DTCR1** and designed compounds **DTCD2** to **DTCD8.**

HOMO electronic cloud was inspected by 'D2' and π-bridge while the LUMO distributions examined to be on 'A' part. Almost similar distribution pattern between LUMO/HOMO was noted for derivatives **DTCD6** and **DTCD7**. All plotted electronic charge distribution patterns unveil that the derivative **DTCD**8 shifts the charge density more significantly among all the designed chromophores. Hence, efficient charge transference occurs through π-spacer in all the derivatives, indicated that these NF compounds could be proficient NLO materials.

3.7. Nonlinear Optical (NLO) properties

The NF compounds show excellent NLO response and find multipurpose applications in telecommunication region and

optoelectronic techniques. The electronic properties of the tailored molecules are determined for the purpose of optical investigations, like linear behavior ($\langle\alpha\rangle$) and non-linear properties (β_{total} and γ_{total}) [7]. By incorporating electron donating substituents and their accepting counterparts at favorable positions of a conjugated structure, the delocalization power of the electrons in any system can be increased. This extended conjugation produce lower transition energy and improves the degree of charge transport which in turn improves the asymmetric division of electrons and may cause promising NLO response of the compounds [55]. In **DTCD2-DTCD8**, delocalization of π-electrons within the phenyl rings was enhanced and C—C π-bond contributed in extended hyper-conjugation of two or more than two phenylic rings. Also, in these investigated compounds, the delocalization was improved by the introduction of fluoro, chloro and cyano substituents which shift electronic density in a better way. In D-A type NLO compounds, π-conjugation generally gives a pathway for the reorganization of electrons under the influence of an applied electric field. Therefore, insertion of a π-linker to connect various suitable 'D' and 'A' moieties has been reported to enhance ICT and consequently, increase of polarizabilities [56]. Additionally, the polarity has shown a tremendous effect on dipole moment *via* enriching the NLO response. Greater dipole moment results from higher difference in electronegativity [57]. The results of entitled chromophores were calculated in *esu* units at M06 functional as shown in Tables 7–10, respectively with their major contributing tensors.

The reference molecule (**DTCR1**) has the lowest linear polarizability ($\langle\alpha\rangle = 1.624 \times 10^{-22}$ *esu*). The powerful 'A' unit along with strong EWGs has enhanced the $\langle\alpha\rangle$ value 1.783×10^{-22}–1.920×10^{-22} *esu* in the designed products (**DTCD2-DTCD8**). **DTCD8** possesses the highest polarizability value of 1.920×10^{-22} *esu* which results in its highest μ_{total} (12.14 *D*). The overall descending trend of μ_{total} for investigated molecules is given as **DTCD8 > DTCD2 > DTCD6 > DTCD4 > DTCD3 > DTCD7 > DTCD5 > DTCR1** with dipole moments of 12.14 > 7.910 > 7.807 > 7.568 > 6.819 > 6.740 > 6.398 > 3.835 *D*, respectively.

The μ_{total} tensors have three components along three axes (μ_x, μ_y and μ_z) (Table 7). Among all the studied compounds, the higher μ_{total} value was seen along Y-axis (μ_y tensor) except **DTCR1** and **DTCD7** which exhibited the highest values along Z-axis (μ_z tensor). In addition to the highest μ_{total}, **DTCD7** also displayed the greatest $\langle\alpha\rangle$ (1.920×10^{-22} *esu*) owing to the occurrence of four —CN groups at 'A' moiety which direct the electronic cloud towards acceptor and makes it powerful electron-capturing molecule. The $\langle\alpha\rangle$ was decreased in the following order: **DTCD8 > DTCD6 > DTCD7 > DTCD5 > DTCD3 > DTCD2 > DTCD4 > DTCR1** with values of $1.920 \times 10^{-22} > 1.870 \times 10^{-22} > 1.860 \times 10^{-22} > 1.815 \times 10^{-22} > 1.789 \times 10^{-22} > 1.783 \times 10^{-22} > 1.779 \times 10^{-22} > 1.624 \times 10^{-22}$ *esu*, respectively. The $\langle\alpha\rangle$ tensors have also three components, *i.e.*, α_{xx}, α_{yy} and α_{zz}, respectively (Table 8). All the molecules exhibited higher values of $\langle\alpha\rangle$ along Z-axis (α_{zz} tensor) signifying greater chances of ICT along the Z -axis.

Moreover, a systematic connection was found between the molecular structures and β_{total} amplitudes. All derivatives expressed significant NLO response (6.926×10^{-28} to 10.58×10^{-28} *esu*) as compared to their reference molecule (1.360×10^{-28} *esu*) (Table 9); this might be because of the change in arrangement from A-π-D-π-A to D1-π-D2-π-A. Moreover, the introduction of electronegative groups (*i.e.,* chloro, fluoro and cyano) on the 'A' moiety also significantly facilitates the ICT, which results in excellent NLO behavior

Table 7 Dipole moment and major contributing tensors of the studied compounds (**DTCR1** and **DTCD2-DTCD8**).

Compounds	μ_x	μ_y	μ_z	μ_{total}
DTCR1	−0.015	−3.760	0.754	3.835
DTCD2	−3.943	6.442	2.347	7.910
DTCD3	−6.458	3.941	−0.204	7.568
DTCD4	−4.852	4.770	0.443	6.819
DTCD5	−6.814	3.445	1.627	7.807
DTCD6	−4.808	4.220	−0.111	6.398
DTCD7	−12.02	−1.623	0.546	12.141
DTCD8	−6.645	0.892	−0.687	6.740

Units in *D*.

Table 8 Linear polarizability and major contributing tensors of the studied compounds.

Compounds	$\alpha_{xx} \times 10^{-22}$	$\alpha_{yy} \times 10^{-22}$	$\alpha_{zz} \times 10^{-23}$	$\alpha_{total} \times 10^{-22}$
DTCR1	2.874	1.469	5.295	1.624
DTCD2	3.061	1.549	7.404	1.783
DTCD3	3.099	1.464	8.027	1.789
DTCD4	3.070	1.374	8.918	1.779
DTCD5	3.094	1.458	8.945	1.815
DTCD6	3.225	1.607	7.793	1.870
DTCD7	3.216	1.570	7.938	1.860
DTCD8	3.349	1.618	7.919	1.920

Units in *esu*.

Table 9 Computed first hyperpolarizability (β_{total}) and major contributing tensors of the studied compounds.

Compounds	$\beta_{xxx} \times 10^{-28}$	$\beta_{xxy} \times 10^{-29}$	$\beta_{xyy} \times 10^{-29}$	$\beta_{yyy} \times 10^{-30}$	$\beta_{xxz} \times 10^{-29}$	$\beta_{yyz} \times 10^{-30}$	$\beta_{xzz} \times 10^{-30}$	$\beta_{yzz} \times 10^{-31}$	$\beta_{zzz} \times 10^{-31}$	$\beta_{total} \times 10^{-28}$
DTCR1	0.034	12.44	−0.016	−27.02	9.281	−0.549	0.313	14.67	11.16	1.360
DTCD2	−7.061	−2.600	1.512	6.242	7.226	1.843	−4.168	−6.451	0.999	6.994
DTCD3	−7.213	1.746	1.756	7.648	4.783	4.921	2.538	8.925	6.217	7.037
DTCD4	−7.103	2.895	1.466	6.692	3.981	4.222	5.376	9.312	0.021	6.926
DTCD5	−7.360	2.528	2.014	16.12	4.258	6.892	5.200	16.56	3.175	7.137
DTCD6	−8.299	0.316	2.173	15.54	8.698	4.465	−4.328	−2.055	7.083	8.179
DTCD7	−9.133	1.539	1.513	−0.509	7.213	0.803	−1.487	−9.242	1.876	9.028
DTCD8	−10.54	−0.872	0.915	−8.776	10.58	−1.577	−7.130	−17.76	5.757	10.58

Units in *esu*.

of derivatives. Owing to the existence of four —CN groups, **DTCD8** shows the highest β_{total} value (10.58×10^{-28} *esu* of β_{total}) as compared to the other designed molecules. The β_{total} values for the investigated compounds were decreased in the following order: **DTCD8** (10.58×10^{-28}) > **DTCD7** (9.028×10^{-28}) > **DTCD6** (8.179×10^{-28}) > **DTCD5** (7.137×10^{-28}) > **DTCD3** (7.037×10^{-28}) > **DTCD2** (6.994×10^{-28}) > **DTCD4** (6.926×10^{-28}) > **DTCR1** (1.360×10^{-28}) in *esu*.

The β_{total} values of **DTCD3** (having one —F) and **DTCD4** (having two —F) were found to be 7.037×10^{-28} and 6.926×10^{-28} *esu*, respectively. In the cases of **DTCD5** (having one —Cl) and **DTCD6** (having two —Cl) the accepting nature of phenyl ring was enhanced. Hence, β_{total} values were shifted from 7.137×10^{-28} *esu* in **DTCD5** to 8.179×10^{-28} *esu* in **DTCD6** due to greater resonance effect of chloro in the latter. **DTCD7** and **DTCD8** exhibited the highest β_{total} values of 9.028×10^{-28} *esu* and 10.58×10^{-28} *esu*, correspondingly, and consequently best NLO response among the whole series of compounds; it is due to the highest -I effect of —CN moieties. The calculated results of $\langle\alpha\rangle$ and β_{total} of studied compounds are appreciably better than urea ($\beta_{total} = 0.372 \times 10^{-30}$ *esu*) which is utilized as a standard molecule to analyze the NLO behavior [58]. The hyperpolarizability values of **DTCR1** and **DTCD2-DTCD8** were observed to be 365.591, 1880.108, 1891.667, 1861.828, 1918.548, 2198.656, 2426.882 and 2844.086 times larger than β_{total} value of the standard urea.

There are nine components of β_{total} tensors which are β_{xxx}, β_{xxy}, β_{xyy}, β_{yyy}, β_{xxz}, β_{yyz}, β_{xzz}, β_{yzz}, β_{zzz} (Table 9). All the investigated molecules have shown the highest amplitude of first hyperpolarizability towards x-axis (β_{xxz} tensor) determining higher possibility of ICT towards X-axis. The descending order of β_{xxz} was found in the following order as **DTCD8 > DTCR1 > DTCD6 > DTCD2 > DTCD7 > DTCD3 > DTCD5 > DTCD4** which show β_{xxz} values of $10.58 \times 10^{-29} > 9.281 \times 10^{-29} > 8.698 \times 10^{-29} > 7.226 \times 10^{-29} > 7.213 \times 10^{-29} > 4.783 \times 10^{-29} > 4.258 \times 10^{-29} > 3.981 \times 10^{-29}$ *esu*, respectively. From Table 9 it is identified that **DTCD8** shows highest β_{xxz} amplitude of 10.58×10^{-29} *esu*.

The above mentioned factors also influence the γ_{total} values of molecules. Table 10 displays the calculated γ_{total} of **DTCR1** and **DTCD2-DTCD8**. Largest γ_{total} value of 8.028×10^{-33} *esu* was observed for **DTCD8**. The overall descending trend of γ_{total} amplitudes was noticed in the following order: **DTCD8 > DTCD7 > DTCD6 > DTCR1 > DTCD2 > DTCD5 > DTCD3 > DTCD4** having γ_{total} values of 8.028×10^{-33}, 6.808×10^{-33}, 6.521×10^{-33}, 5.993×10^{-33}, 5.539×10^{-33}, 5.446×10^{-33}, 5.417×10^{-33} and 5.275×10^{-33} *esu*, respectively. The γ_{total} also has three components of tensors (γ_x, γ_y and γ_z) (Table 10). Among all the entitled molecules, γ_x expresses the greatest amplitude of γ_{total} along X-axis indicating higher probability of charge transfer along X-axis. **DTCD8** exhibited the highest γ_x amplitude (7.841×10^{-33}*esu*) among all the designed molecules. To understand the dispersion factor in NLO behavior of our studied compounds, we also performed NLO analysis at dispersion functional B3LYP-GD3BJ/6-311G(d,p) and important results were displayed in Table S33, while their major contributing tensors were tabulated in Tables S33–S37, respectively. The results shows the magnitude of μ_{total}, $\langle\alpha\rangle$, β_{total} and γ_{total} was almost same at both M06-2X and B3LYP-GD3BJ/6-311G(d,

Table 10 Computed second hyperpolarizability (γ_{total}) and major contributing tensors of the investigated compounds.

Compounds	$\gamma_x \times 10^{-33}$	$\gamma_y \times 10^{-35}$	$\gamma_z \times 10^{-35}$	$\gamma_{total} \times 10^{-33}$
DTCR1	5.834	11.73	4.146	5.993
DTCD2	5.425	6.444	4.964	5.539
DTCD3	5.316	5.289	4.822	5.417
DTCD4	5.180	4.804	4.659	5.275
DTCD5	5.318	7.825	5.006	5.446
DTCD6	6.352	10.42	6.422	6.521
DTCD7	6.666	8.127	6.090	6.808
DTCD8	7.841	11.15	7.565	8.028

Units in *esu*.

p) functional. So, it can be concluded that the electron capturing nature of 'A' moieties performs a crucial part in yielding excellent NLO properties in the derivatives.

4. Conclusion

A series of compounds (**DTCD2-DTCD8**) was designed from a NF molecule (**DTCR1**) by altering the architecture of the molecule from A-π-D2-π-A to D1-π-D2-π-A. It was found that acceptors have a significant effect on the arrangement and improve the NLO response of designed molecules over the reference molecule. **DTCD2-DTCD8** manifested the greater absorption, less transitional energy, and oscillation strength values as compared to **DTCR1**. The highest bathochromic shift (λ_{max} = 524.043 *nm*) was shown by **DTCD8** as compared to all other studied molecules. The energy gap (4.221 *eV*) of **DTCR1** was lowered to 3.970–3.603 *eV* in **DTCD2-DTCD8** and among all derivatives lowest E_{gap} (3.603 *eV*) was found in **DTCD8**. Moreover, DOS results also supported the FMOs findings that charge transference occurred from HOMO to LUMO in an efficient way. NLO findings reveal that significant $\langle\alpha\rangle$, β_{total} and γ_{total} values as 1.920×10^{-22} *esu*, 10.58×10^{-28} *esu* and 8.028×10^{-33} *esu*, respectively have been investigated in **DTCD8** as compared to **DTCR1** and other derivatives. Promising NLO results for **DTCD8** can be achieved due to the powerful electron-withdrawing (—CN) groups. Moreover, NBOs findings reveal that hyperconjugation enhances the stability of **DTCD2-DTCD8** which was further supported by the results of GRPs. TDM analysis illustrated that electronic transitions take place from "D" to "A" through π-linker. Experimental researchers might be motivated by efficient NLO responses, and our designed compounds can be considered in other useful applications.

CRediT authorship contribution statement

Muhammad Khalid: Methodology, Software, Project administration. **Zubaria Saeed:** Data curation, Formal analysis, Validation. **Iqra Shafiq:** Data curation, Formal analysis. **Muhammad Adnan Asghar:** Resources, Software, Supervision. **Ataualpa Albert Carmo Braga:** Data curation, Formal analysis, Validation. **Saad M. Alshehri:** Conceptualization, Methodology, Software. **Muhammad Safwan Akram:** Conceptualization, Methodology. **Suvash Chandra Ojha:** Conceptualization, Methodology, Supervision.

Declaration of Competing Interest

The authors declare that they have no known competing financial interests or personal relationships that could have appeared to influence the work reported in this paper.

Acknowledgments

Dr. Muhammad Khalid gratefully acknowledges the financial support of HEC Pakistan (project no. 20-14703/NRPU/R&D/HEC/2021). A.A.C.B. acknowledges the financial support of the São Paulo Research Foundation (FAPESP) (Grants 2014/25770-6 and 2015/01491-3), the Conselho Nacional de Desenvolvimento Científico e Tecnológico (CNPq) of Brazil for academic support (Grant 309715/2017-2), and Coordenação de Aperfeiçoamento de Pessoal de Nível Superior – Brasil (CAPES) that partially supported this work (Finance Code 001). The authors thank the Researchers Supporting Project number (RSP2023R29), King Saud University, Riyadh, Saudi Arabia. S.C.O. acknowledges the support from the doctoral research fund of the Affiliated Hospital of Southwest Medical University.

Appendix A. Supplementary material

Supplementary material to this article can be found online at https://doi.org/10.1016/j.jscs.2023.101683.

References

[1] F. Zafar, M.Y. Mehboob, R. Hussain, A. Hussain, T. Hassan, M. Rashid, M.N. Shahi, End-capped engineering of truxene core based acceptor materials for high performance organic solar cells: theoretical understanding and prediction, Opt. Quantum Electron. 53 (2021) 1–24.

[2] G.W. Ejuh, N. Samuel, T.N. Fridolin, N.J. Marie, Computational determination of the Electronic and Nonlinear Optical properties of the molecules 2-(4-aminophenyl) Quinoline, 4-(4-aminophenyl) Quinoline, Anthracene, Anthraquinone and Phenanthrene, Mater. Lett. 178 (2016) 221–226.

[3] C. Wang, Z. Zhang, Y. Wang, Quinacridone-based π-conjugated electronic materials, J. Mater. Chem. C 4 (2016) 9918–9936.

[4] J. Indira, P.P. Karat, B.K. Sarojini, Growth, characterization and nonlinear optical property of chalcone derivative, J. Cryst. Growth 242 (2002) 209–214.

[5] M.R.S.A. Janjua, Non-linear Optical response of Phenoxazine-based Dyes: Molecular Engineering of Thiadiazole Derivatives as π-spacers, J. Mex. Chem. 61 (2017) 260–265.
[6] A. Mahmood, Y. Sandali, J.-L. Wang, Easy and fast prediction of green solvents for small molecule donor-based organic solar cells through machine learning, Phys. Chem. Chem. Phys. 25 (2023) 10417–10426.
[7] P.S. Halasyamani, W. Zhang, Viewpoint: Inorganic Materials for UV and Deep-UV Nonlinear-Optical Applications, Inorg. Chem. 56 (2017) 12077–12085.
[8] A. Mahmood, S.U.D. Khan, U.A. Rana, M.R.S.A. Janjua, M. H. Tahir, M.F. Nazar, Y. Song, Effect of thiophene rings on UV/visible spectra and non-linear optical (NLO) properties of triphenylamine based dyes: a quantum chemical perspective, J. Phys. Org. Chem. 28 (2015) 418–422.
[9] R. Mahmood, M.R.S.A. Janjua, S. Jamil, DFT molecular simulation for design and effect of core bridging acceptors (BA) on NLO response: first theoretical framework to enhance nonlinearity through BA, J. Clust. Sci. 28 (2017) 3175–3183.
[10] A. Broo, Electronic structure of donor-spacer-acceptor molecules of potential interest for molecular electronics. II. Donor-σ spacer-acceptor, Chem. Phys. 169 (1993) 151–163.
[11] M. Wielopolski, J.H. Kim, Y.S. Jung, Y.J. Yu, K.Y. Kay, T.W. Holcombe, S.M. Zakeeruddin, M. Grätzel, J.-E. Moser, Position-dependent extension of π-conjugation in D-π-A dye sensitizers and the impact on the charge-transfer properties, J. Phys. Chem. C 117 (2013) 13805–13815.
[12] M.R.S.A. Janjua, A. Mahmood, M.F. Nazar, Z. Yang, S. Pan, Electronic absorption spectra and nonlinear optical properties of ruthenium acetylide complexes: a DFT study toward the designing of new high NLO response compounds, Acta Chim. Slov. 61 (2014) 382–390.
[13] J. Zhang, H.S. Tan, X. Guo, A. Facchetti, H. Yan, Material insights and challenges for non-fullerene organic solar cells based on small molecular acceptors, Nat. Energy 3 (2018) 720–731.
[14] Y. Zhang, G. Li, Functional Third Components in Nonfullerene Acceptor-Based Ternary Organic Solar Cells, Acc. Mater. Res. 1 (2020) 158–171.
[15] L. Duan, N.K. Elumalai, Y. Zhang, A. Uddin, Progress in non-fullerene acceptor based organic solar cells, Sol. Energy Mater. Sol. Cells 193 (2019) 22–65.
[16] P. Cheng, G. Li, X. Zhan, Y. Yang, Next-generation organic photovoltaics based on non-fullerene acceptors, Nat. Photonics 12 (2018) 131–142.
[17] R. Ketavath, K.P.K. Naik, S.G. Ghugal, N.K. Katturi, T. Swetha, V.R. Soma, B. Murali, Metal-free carbazole scaffold dyes as potential nonlinear optical phores: molecular engineering, J. Mater. Chem. C 8 (2020) 16188–16197.
[18] D. Jiang, S. Chen, Z. Xue, Y. Li, H. Liu, W. Yang, Y. Li, Donor–acceptor molecules based on benzothiadiazole: Synthesis, X-ray crystal structures, linear and third-order nonlinear optical properties, Dyes Pigm. 125 (2016) 100–105.
[19] A. Dhiman, L. Giribabu, R. Trivedi, π-Conjugated Materials Derived From Boron-Chalcogenophene Combination. A Brief Description of Synthetic Routes and Optoelectronic Applications, Chem. Rec. 21 (2021) 1738–1770.
[20] D.W. Lee, T. Kim, M. Lee, An amphiphilic pyrene sheet for selective functionalization of graphene, Chem. Commun. 47 (2011) 8259–8261.
[21] M.J. Frisch, G.W. Trucks, H.B. Schlegel, G.E. Scuseria, M.A. Robb, J.R. Cheeseman, G. Scalmani, V. Barone, G.A. Petersson, H. Nakatsuji, Gaussian 16 Revision C. 01. 2016; Gaussian Inc, Wallingford CT. 421 (2016).
[22] K.H. Lemke, T.M. Seward, Thermodynamic properties of carbon dioxide clusters by M06–2X and dispersion-corrected B2PLYP-D theory, Chem. Phys. Lett. 573 (2013) 19–23.
[23] J.E. Del Bene, D.H. Aue, I. Shavitt, Stabilities of hydrocarbons and carbocations. 1. A comparison of augmented 6–31G, 6–311G, and correlation consistent basis sets, J. Am. Chem. Soc. 114 (1992) 1631–1640.
[24] L.G. Zhuo, W. Liao, Z.X. Yu, A Frontier Molecular Orbital Theory Approach to Understanding the Mayr Equation and to Quantifying Nucleophilicity and Electrophilicity by Using HOMO and LUMO Energies, Asian J. Org. Chem. 1 (2012) 336–345.
[25] E. Tanış, N. Çankaya, S. Yalçın, Synthesis, Characterization, Computation of Global Reactivity Descriptors and Antiproliferative Activity of N-(4-nitrophenyl)Acrylamide, Russ. J. Phys. Chem. B 13 (2019) 49–61.
[26] Y. Li, C.A. Ullrich, Time-dependent transition density matrix, Chem. Phys. 391 (2011) 157–163.
[27] F. Wang, D.P. Landau, Efficient, Multiple-Range Random Walk Algorithm to Calculate the Density of States, Phys. Rev. Lett. 86 (2001) 2050–2053.
[28] K. Kahouli, A.B.J. Kharrat, S. Chaabouni, Optical properties analysis of the new (C9H14N)3BiCl6 compound by UV–visible measurements, Indian J. Phys. 95 (2021) 2797–2805.
[29] E. Runge, E.K.U. Gross, Density-Functional Theory for Time-Dependent Systems, Phys. Rev. Lett. 52 (1984) 997–1000.
[30] M. Cossi, N. Rega, G. Scalmani, V. Barone, Energies, structures, and electronic properties of molecules in solution with the C-PCM solvation model, J. Comput. Chem. 24 (2003) 669–681.
[31] Glendening, NBO 6.0: Natural bond orbital analysis program – Google Scholar [WWW Document], n.d. URL. 34 (2013) 1429–1437.
[32] R.D. Dennington, T.A. Keith, J.M. Millam, GaussView 5.0, 20, Gaussian Inc., Wallingford, 2008.
[33] M.D. Hanwell, D.E. Curtis, D.C. Lonie, T. Vandermeersch, E. Zurek, G.R. Hutchison, Avogadro: an advanced semantic chemical editor, visualization, and analysis platform, J. Cheminformat. 4 (2012) 1–17.
[34] G.A. Zhurko, D.A. Zhurko, ChemCraft, version 1.6, URL: Http://Www, Chemcraftprog. Com. (2009).
[35] N.M. O'boyle, A.L. Tenderholt, K.M. Langner, Cclib: a library for package-independent computational chemistry algorithms, J. Comput. Chem. 29 (2008) 839–845.
[36] T. Lu, F. Chen, Multiwfn: a multifunctional wavefunction analyzer, J. Comput. Chem. 33 (2012) 580–592.
[37] B. Civalleri, C.M. Zicovich-Wilson, L. Valenzano, P. Ugliengo, B3LYP augmented with an empirical dispersion term (B3LYP-D*) as applied to molecular crystals, CrstEngComm 10 (2008) 405–410.
[38] A. Alparone, Linear and nonlinear optical properties of nucleic acid bases, Chem. Phys. 410 (2013) 90–98.
[39] H.A. Kurtz, J.J.P. Stewart, K.M. Dieter, Calculation of the nonlinear optical properties of molecules, J. Comput. Chem. 11 (1990) 82–87.
[40] K.B. Lipkowitz, D.B. Boyd, Reviews in Computational Chemistry 7(7) (2009) 67.
[41] A. Plaquet, M. Guillaume, B. Champagne, F. Castet, L. Ducasse, J.-L. Pozzo, In silico optimization of merocyanine-spiropyran compounds as second-order nonlinear, Phys. Chem. Chem. Phys. 10 (2008) 6223–6232.
[42] J. Liao, P. Zheng, Z. Cai, S. Shen, G. Xu, H. Zhao, Y. Xu, Construction of simple and low-cost acceptors for efficient non-fullerene organic solar cells, Org. Electron. 89 (2021) 106026.
[43] M.R.S.A. Janjua, Quantum chemical design and prediction that complements understanding: How do the transition metals enhance the CO2 sensing ability of inorganic Mg12O12 nanoclusters?, J Phys. Chem. Solid 167 (2022) 110789.
[44] M. Haroon, M.R.S.A. Janjua, Prediction of NLO response of substituted organoimido hexamolybedate: First theoretical

framework based on p-anisidine adduct [Mo6O18(p-MeOC6H4N)]2-, Mater. Today Commun. 26 (2021) 101880.
[45] S. Namuangruk, R. Fukuda, M. Ehara, J. Meeprasert, T. Khanasa, S. Morada, T. Kaewin, S. Jungsuttiwong, T. Sudyoadsuk, V. Promarak, D-D- π–A-Type organic dyes for dye-sensitized solar cells with a potential for direct electron injection and a high extinction coefficient: synthesis, characterization, and theoretical investigation, J. Phys. Chem. C 116 (2012) 25653–25663.
[46] M.I. Nan, E. Lakatos, G.I. Giurgi, L. Szolga, R. Po, A. Terec, S. Jungsuttiwong, I. Grosu, J. Roncali, Mono-and di-substituted pyrene-based donor-π-acceptor systems with phenyl and thienyl π-conjugating bridges, Dyes Pigm. 181 (2020) 108527.
[47] P.K. Chattaraj, D.R. Roy, Update 1 of: electrophilicity index, Chem. Rev. 107 (2007) PR46–PR74.
[48] C. Anbuselvan, J. Jayabharathi, V. Thanikachalam, G. Tamilselvi, Physico-chemical studies on some fluorescence sensors: DFT based ESIPT process, Spectrochim. Acta A Mol. Biomol. Spectrosc. 97 (2012) 125–130.
[49] N. Sadlej-Sosnowska, Application of natural bond orbital analysis to delocalization and aromaticity in C-substituted tetrazoles, J. Org. Chem. 66 (2001) 8737–8743.
[50] N.R. Rajagopalan, P. Krishnamoorthy, K. Jayamoorthy, S. Manikandan, Synthesis, Characterization, Thermal Analysis, Nucleation Kinetics and DFT Studies of Bis(thiourea) Antimony Tribromide as Potential NLO Material: Comparison of Experimental and Computational Studies, J. Inorg. Organomet. Polym. 27 (2017) 1457–1465.
[51] M. Yahya, G. Kurtay, A.R. Suvitha, On the viability of divergent donor moieties in malononitrile-based donor-π-acceptor NLO active materials: A DFT/TD-DFT study, J. Phys. Org. Chem. 35 (2022) e4403.
[52] A. Dkhissi, Excitons in organic semiconductors, Synth. Met. 161 (2011) 1441–1443.
[53] M. Ans, J. Iqbal, K. Ayub, E. Ali, B. Eliasson, Spirobifluorene based small molecules as an alternative to traditional fullerene acceptors for organic solar cells, Mater. Sci. Semicond. Process. 94 (2019) 97–106.
[54] A. Bibi, S. Muhammad, S. UrRehman, S. Bibi, S. Bashir, K. Ayub, M. Adnan, M. Khalid, Chemically modified quinoidal oligothiophenes for enhanced linear and third-order nonlinear optical properties, ACS Omega 6 (2021) 24602.
[55] J. Jayabharathi, V. Thanikachalam, K. Jayamoorthy, M. Venkatesh Perumal, Computational studies of 1,2-disubstituted benzimidazole derivatives, Spectrochim. Acta A Mol. Biomol. Spectrosc. 97 (2012) 131–136.
[56] B.S. Mendis, K.N. de Silva, A comprehensive study of linear and non-linear optical properties of novel charge transfer molecular systems, J. Mol. Struct. (Thoechem) 678 (2004) 31–38.
[57] I. Manikandan, M.V. Perumal, K. Jayamoorthy, Synthesis, characterization, physico-chemical and DFT studies of potential organic NLO materials: experimental and theoretical combined study, Silicon 11 (2019) 425–435.
[58] D.P. Shelton, J.E. Rice, Measurements and calculations of the hyperpolarizabilities of atoms and small molecules in the gas phase, Chem. Rev. 94 (1994) 3–29.